Fredy FLORES-BAHAMONDE[1], Hugo VALDERRAMA-BLAVI[1], Josep Maria BOSQUE-MONCUSI[1], Luis MARTINEZ-SALAMERO[1], Antonio LEON-MASICH[1], Jose Antonio BARRADO[1]

GAEI Laboratory, University Rovira i Virgili (1)

Single-Phase PFC for Three-Phase Wind Generator, a Modular Approach.

***Abstract**. To adapt a 3-phase wind alternator to a variable DC-bus, a modular solution based on single-phase Boost-based PFC's is proposed. Nevertheless, oost modules must be adapted to operate with non-isolated sources, like 3-4 wire, 3-phase generators. Magnetic coupling is introduced to enhance the isolation among phases, reducing also converter losses and size. Sliding mode approach has been applied to verify that independent regulation of all phase modules was possible. To confirm the theoretical analysis A 1.5 kW prototype was built for verification.*

***Streszczenie.** W artykule zaproponowano układ modułowy do sprzęgania generatora wiatrowego z regulowanym obwodem prądu stałego oparty na jednofazowym układzie korekcji współczynnika mocy typu boost PFC. Układ boost został zaadoptowany do pracy ze źródłami nieizolowanymi takimi jak trzy- i czteroprzewodowe generatory trójfazowe. Zaprezentowano sprzężenie magnetyczne poprawiające izolację międzyfazową redukującą także straty w przekształtniku oraz jego wymiary. Zastosowano sterowanie ślizgowe w celu wykazania możliwości niezależnego sterowania we wszystkich fazach. Zbudowano prototyp o mocy 1,5 kW do weryfikacji eksperymentalnej wyników analiz teoretycznych.(**Jednofazowy układ PFC do trójfazowych generatorów wiatrowych, rozwiązanie modułowe**)*

Keywords: Modular system, Redundancy, Single-phase PFC rectifier, Wind generator
Słowa kluczowe: System modułowy, redundancja, prostownik z korekcją współczynnika mocy, generator wiatrowy

Introduction

Greenhouse emissions can be significantly reduced using small renewable generation sources. Energy production optimization requires improvements in generators, conversion stages, and transport networks. Distributed generation system (DGs) development can contribute to generate electricity with lower transport losses and low pollution.

Nevertheless, the main interest of DGS's is to improve the distribution efficiency approaching generation sites to the consumption centers. In this context, big power plants far from consumers imply excessive transport costs, so DGS are oriented to low power production centers, frequently based on renewable energies.

Common renewable-based systems considering the electrical grid an infinite sink, have a grid penetration limit around 25%, because can cause grid instability. Today, small DGS normally include storage devices and different energy sources to create an energy reservoir. As a result, these systems can implement now, active grid-cooperation promoting their expansion [1].

A distributed generation system is under development in our laboratory, see Fig. 1. A variable voltage DC Bus, (270-370 V) is the system core.

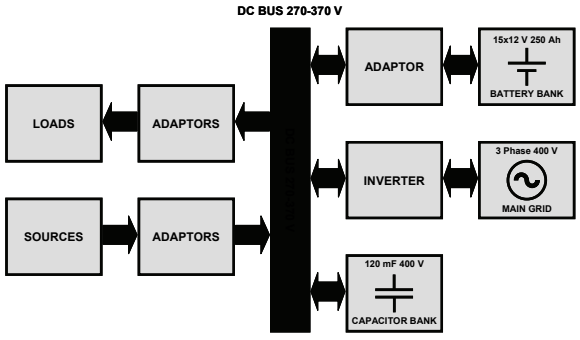

Fig.1. GAEI Laboratory DC-Microgrid

The use of a DC-micogrid, as shown in Fig. 1, allows manage many sources with only a 6 kW inverter and a single grid connection point (PCC). All the generators, storage elements, and loads are connected to the DC-bus through an adaptor circuit [2]. This adaptor can make many different functions depending on the bus architecture.

To design adaptors, modularity and redundancy concept for DC-microgrid, can help to simplify the integration of many sources [3]. To integrate diverse elements to the small-grid, adaptors design can be a very complicated issue, specifically for three-phase power sources.

PFC analysis

Design of high efficiency PFC converters with reduced harmonic content, low EMI, cost, and size continues to be an interesting research subject. Many different PFC approaches assuring a good sinusoidal input current and output voltage regulation can be found in the literature.

Boost converter derived topologies are widely used at PFC applications. For three-phase system, due its good performances, six-switch and Vienna rectifiers are very common. However, for modular approaches, only the Vienna rectifier is considered as modular single-phase PFC.

Different types of Vienna rectifiers can be found. This rectifier does not require a large capacitance and the switches are subject to only 50% of the high bus voltage, reducing the stress. Despite this advantages, the control of Vienna rectifier is still complex [4-5].

As modular topology, single-phase PFC rectifier is the most common circuit used for many authors in both, telecommunication and power electronics. The single-phase rectifier is more and more popular, due the modularity and easy implementation without complex control scheme. This design complies with two important advantages, good shape input-currents and several harmonics standards.

The main problem of single-phase PFC rectifier appears when input sources are not floating, as three-phase conventional 3-4 wire generator. The direct connection of the PFC outputs through a common DC-link capacitor implies interaction among the stages, unbalancing the system.

Commonly, each single-phase PFC is followed by a dc/dc converter with insulation transformer, shown in Fig. 2. This solution decouples each unit, and can work also with unbalanced main sources and distorted input current. Although, this solution keeps the system balance avoiding the interaction among the stages, reduces the converter efficiency due the high number of semiconductors and the transformer leakage losses. Different control techniques

was been developed to increase the efficiency, but imply complex control schemes [4-6-7].

References [7-8] propose a second solution to improve isolation among stages. Although in this case, Boost converter topology is retained, and the diode and the inductor, are both split, as explained in the next section.

The work presented in this paper continues that research work, improving the isolation performance using coupled inductors.

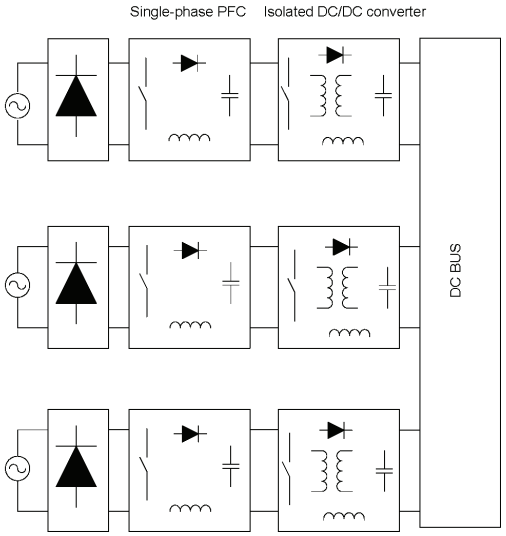

Fig.2. Single-phase rectifier with isolated DC/DC converter

Circuit Development

In the previous section, a modification of a common boost to keep the input phases balanced is mentioned. In this section, we explain the interaction problem appearing in the modular PFC when the single-phase modules are connected to a 3-4 wire 3-phase generator, instead of being connected to three floating generator (six-wire connection). Next, the solutions found in the literature are discussed, and after, the improvements proposed in this work are clearly presented. An experimental 1.5 kW prototype, presented in Section V, will prove the system performances.

Previous System

The interaction problems can be easily understood analyzing the circuits shown in Fig. 3. Here, for three-phase four-wire input system, three single-phase PFC rectifiers are connected to the same output DC-link capacitor without isolation. A partial solution to this problem implies various steps. First, the diode must be split, and then the same applies to the inductor.

To simplify the explanation, only two of the three single-phase PFC rectifiers are considered, see Fig 3a. In this circuit, any switches combination can be made. To analyze the circuit, let's consider a case where the voltage phases have opposite sign ($e_1>0$ and $e_2<0$) and both switches are in the ON state. In this moment, node B (fig. 3) is more negative than e_1 neutral wire (N_1), because e_2 has a negative voltage. This blocks D_4 diode in the upper stage, and then, the upper converter current goes through the second converter.

This first interaction problem can be partially solved inserting a second freewheeling diode D1b as can be seen in Fig. 3b. As this diode is reverse biased, the current cannot go through the second converter, and goes through the first one.

Until now, we have solved the interaction problem while the mosfets are both at ON-state. Next case to examine is when both switches are in the OFF-state. This case is shown at Fig. 3b. In this moment, B node is still more negative than N_1 wire, diodes D_4 and D_{1b} are blocked, and the current of the upper stage returns through the second converter again. To solve that, a second inductor L_{1b} is placed between the active switch and D_4, forcing the conduction of diode D_{1b}, see Fig. 3c.

If these two corrections are applied to all boost inductors, and freewheeling diodes, each input current should return through its own stage, balancing theoretically the system [7-8].

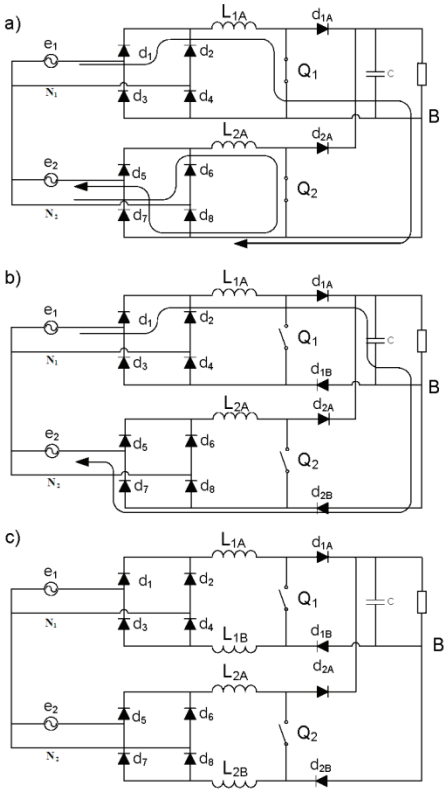

Fig.3. Single-Phase PFC converter, (a) Common Boost. (b) Boost with diode split. (c) Boost with diode and inductor split

Final Proposed circuit

To enhance the effect of the split inductor, we propose to couple the original boost inductor and the second one, as can be seen in the single-phase boost circuit in Fig.4. With the coupled inductor, current ripple, cost, and weight can be reduced. Besides, there is a transformer effect, forcing the system to keep balanced.

Coupled inductors have an important role in power converters. Many authors used coupled inductors to correct non-minimum phase response in the boost cell and similar converters [9-10].

Others [11-12] used inductor coupling to get ideal zero current-ripple in some DC-DC converters. In fact, the induced voltage effect caused a significant ripple reduction, being the ripple slope is related to the coupling factor K value. Ripple reduction has also other positive effects like EMI reduction. Higher efficiency can also be achieved because the number of magnetic cores is halved. Besides, due to a reduced ripple, the RMS values of the currents decreases, and then the conduction losses. Nevertheless, our system is not working at fixed frequency, because the control-loop is based on sliding mode approach. In that case, ripple is determined by the hysteresis band controller, so instead of ripple amplitude reduction, the main effect of coupling is switching frequency reduction.

As presented in the next section, if coupling is perfect and both inductors are equal, the equivalent input inductance is increased by a factor 4. Therefore, in our case, the switching losses are divided also by four.

On other hand, under the same hypothesis, the coupled inductors behave like a transformer with a turns ratio of 1. This means that both inductor currents i_{LA} and i_{Lb}, have to be equal, enhancing the balancing effect of the previously explained split or second inductor.

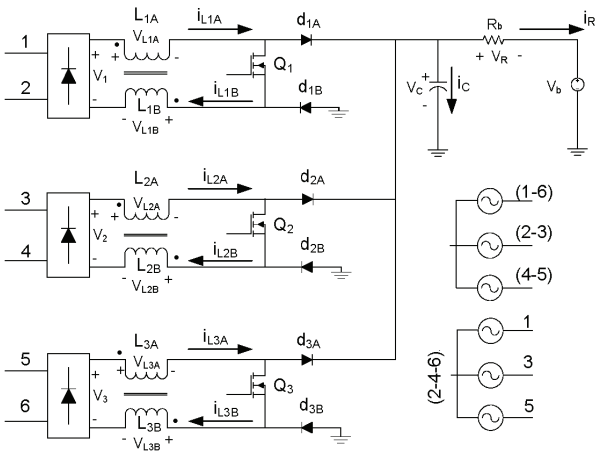

Fig.4. Single-Phase three-phase PFC converter proposed circuit

Circuit Analysis and Control

Circuit in Fig.4 has three boost cells connected in parallel, sharing the output capacitor. Interaction among stages has been apparently solved but, dynamic responses of each converter could be coupled through the output common capacitor. In this section we will prove that independent phase control is possible even sharing the output capacitor. Therefore single phase analysis could be sufficient to describe the circuit operation.

Single-Phase Circuit State-space Model

Fig.5 shows the electrical model of two coils magnetically coupled. The boost converter is a variable structure system, where the switch action distinguishes two circuit topologies, as shown in fig. 7a to 7c. For control purposes, a binary signal u(t)={0,1} is used to indicate each topology, where ON topology is associated to u(t)=1.

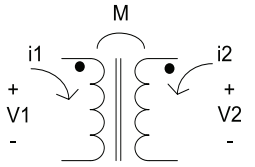

$$V_1 = L_1 \cdot \frac{di_1}{dt} + M \cdot \frac{di_2}{dt}$$

$$V_2 = L_2 \cdot \frac{di_2}{dt} + M \cdot \frac{di_1}{dt}$$

Fig.5. Electrical Model of Coupled inductor

In the circuits of Fig.6a to 6c, V_b is the DC-Bus voltage, the input generator and the full-bridge are replaced by a voltage source V_1, and finally R_b, L_1 and C are the remaining circuit parameters, where $L_1=L_{1A}=L_{1B}$. According to the circuit topologies, the state equations are:

(1) $$\overset{o}{X}_{ON} = \begin{bmatrix} 0 & 0 \\ 0 & -1/R_b C \end{bmatrix} \cdot \begin{bmatrix} i_L \\ v_c \end{bmatrix} + \begin{bmatrix} V_1/4L_1 \\ V_b/R_b C \end{bmatrix}$$

(2) $$\overset{o}{X}_{OFF} = \begin{bmatrix} 0 & -1/4L_1 \\ 1/C & -1/R_b C \end{bmatrix} \cdot \begin{bmatrix} i_L \\ v_c \end{bmatrix} + \begin{bmatrix} V_1/4L_1 \\ V_b/R_b C \end{bmatrix}$$

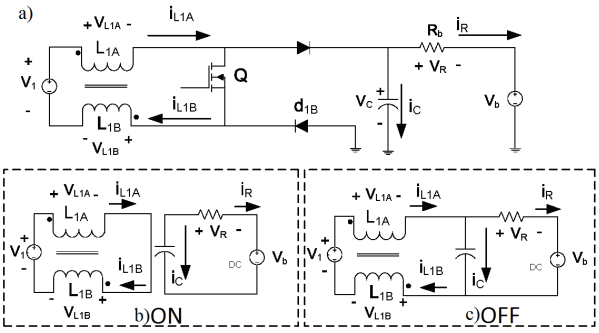

Fig.6. Circuital scheme of Single Phase Converter with coupled inductor. (a) On State (b) OFF State

Full Circuit Analysis

Considering the full circuit of fig. 5, the three switches are controlled independently, and eight possible switching states can appear. The control signals of switches Q_1, Q_2, Q_3, are respectively u_a, u_b, u_c , where $\{u_a, u_b, u_c\}=\{0,1\}$.

After analyzing the eight circuit topologies, it has been found that the dynamic matrix A_{abc} depends on the circuit topology, but the excitation matrix is always the same. The state vector is given as (3), equation (4) describes each topology, and (5) gives the values of A_{abc} and B.

(3) $$X^T = \left[i_{L1}, \quad i_{L2}, \quad i_{L3}, \quad V_C \right]^T$$

(4) $$\overset{o}{X} = A_{abc} \cdot X + B$$

(5) $$A_{abc} = \begin{bmatrix} 0 & 0 & 0 & \frac{u_a - 1}{4L} \\ 0 & 0 & 0 & \frac{u_b - 1}{4L} \\ 0 & 0 & 0 & \frac{u_c - 1}{4L} \\ \frac{1-u_a}{C} & \frac{1-u_b}{C} & \frac{1-u_c}{C} & \frac{-1}{R_b C} \end{bmatrix} \qquad B = \begin{bmatrix} \frac{V_1}{4L} \\ \frac{V_2}{4L} \\ \frac{V_3}{4L} \\ \frac{V_b}{R_b C} \end{bmatrix}$$

By multiplying each topology equation by its activation ffunction, a converter full-time model can be found.

(6)
$$\begin{aligned} &\left[\overset{o}{X} = \left(A_{000} \cdot x + B \right) \right] \cdot \left(1-u_a\right) \cdot \left(1-u_b\right) \cdot \left(1-u_c\right) \\ &+ \left[\overset{o}{X} = \left(A_{001} \cdot x + B \right) \right] \cdot \left(1-u_a\right) \cdot \left(1-u_b\right) \cdot u_c \\ &+ \left[\overset{o}{X} = \left(A_{010} \cdot x + B \right) \right] \cdot \left(1-u_a\right) \cdot u_b \cdot \left(1-u_c\right) \\ &+ \left[\overset{o}{X} = \left(A_{011} \cdot x + B \right) \right] \cdot \left(1-u_a\right) \cdot u_b \cdot u_c \\ &+ \left[\overset{o}{X} = \left(A_{100} \cdot x + B \right) \right] \cdot u_a \cdot \left(1-u_b\right) \cdot \left(1-u_c\right) \\ &+ \left[\overset{o}{X} = \left(A_{101} \cdot x + B \right) \right] \cdot u_a \cdot \left(1-u_b\right) \cdot u_c \\ &+ \left[\overset{o}{X} = \left(A_{110} \cdot x + B \right) \right] \cdot u_a \cdot u_b \cdot \left(1-u_c\right) \\ &+ \left[\overset{o}{X} = \left(A_{111} \cdot x + B \right) \right] \cdot u_a \cdot u_b \cdot u_c \\ &\overset{o}{X} = f\left(X\right) + g_a\left(X\right) \cdot u_a + g_b\left(X\right) \cdot u_b + g_c\left(X\right) \cdot u_c \end{aligned}$$

where $f(X)$, $g_a(X)$, $g_b(X)$, and $g_c(X)$ are given by (7)

(7)
$$f(X) = A_{000}\,X + B$$
$$g_a(X) = \left[A_{100} - A_{000}\right]\cdot X$$
$$g_b(X) = \left[A_{010} - A_{000}\right]\cdot X$$
$$g_c(X) = \left[A_{001} - A_{000}\right]\cdot X$$

After analyzing the model, it can be easily deduced that we have a bilinear system with three control inputs, where each current is affected only by the respective control input, whereas the capacitor voltage is affected by the three.

Sliding Mode Control Law

To assure unity power factor, LFR concept is used. According to that, the generator will see the converter like three resistors, one per phase, and each input current must be in phase with the corresponding input voltage.

(8)
$$S(X) = \left[i_{L1} - g_1 V_1,\quad i_{L2} - g_2 V_2,\quad i_{L3} - g_3 V_3,\quad 0\right] = 0$$

The equivalent control is obtained in (9). Considering the system matrices, the equivalent control is given by (10) where all the transversality conditions are satisfied.

(9)
$$\overset{o}{S} = \nabla S(X)\cdot\overset{o}{X} = \nabla S\cdot\left(f(X) + g_a(X)\cdot u_a + \ldots\right.$$
$$\left.\ldots + g_b(X)\cdot u_b + g_c(X)\cdot u_c\right) = 0$$

(10)
$$u_{eq} = \left[1 - \frac{V_1}{V_C},\quad 1 - \frac{V_2}{V_C},\quad 1 - \frac{V_3}{V_C}\right]$$

The ideal sliding dynamics (11) is obtained considering the surface constraints and substituting the equivalent control in the bilinear expression (6) [13]. Realize that the capacitor voltage dynamics is non linear, and the system dynamics is reduced from four to first order.

From the equilibrium point, at zero bus impedance R_b=0, the capacitor and the bus voltage are the same. If there is no DC-Bus (V_b=0), all the generated power is delivered directly to the "converter load" R_b, and the sliding motions only will exists while V_C>max(V_1,V_2,V_3).

(11)
$$\begin{cases} i_{L1} = g_1 V_1, \quad i_{L2} = g_2 V_2, \quad i_{L3} = g_3 V_3 \\ \overset{o}{V}_C = \dfrac{g_1 V_1^2 + g_2 V_2^2 + g_3 V_3^2}{C V_C} + \dfrac{V_b - V_C}{R_b C} \end{cases}$$

(12)
$$V_C^*\left(R_b \to 0\right) = V_b$$
$$V_C^*\left(V_b \to 0\right) = \sqrt{R_b\left(g_1 V_1^2 + g_2 V_2^2 + g_3 V_3^2\right)}$$

By linearizing capacitor dynamics around the equilibrium point, the local stability can be easily verified. There is a first order pole placed in the left-side of the s-plane

(13)
$$s = -\left[\frac{g_1 V_1^2 + g_2 V_2^2 + g_3 V_3^2}{C V_C^{*2}} + \frac{1}{R_b C}\right]$$

Experimental Results

To match a 3-phase wind generator with the microgrid DC voltage, 270 V<V_b<370 V, a prototype has been developed. The passive components are L=150 μH, C=33 μF. The DC-Bus circuit can be appreciated in Fig.7. The bus is supplied from two power-supplies, connected in series, with the output current limited to 20 A. The first one gives 270 V, and the second, the remaining voltage. A blocking diode avoids inverse currents to the power-supplies that may cause their destruction. The bus has a load of R_L=60 Ω, this means 1.7 kW or 5.33 A at 320 V, an impedance of R_b=50 mΩ, and finally a capacitor bank of C_b=28,200 μF.

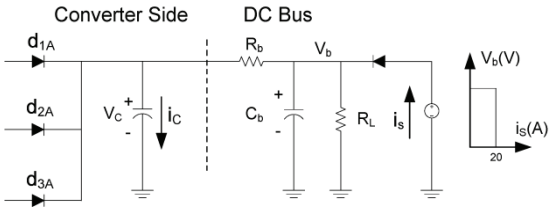

Fig.7. Converter Connection with Test DC-Bus

Photograph in Fig.8 depicts the prototype, the DC-Bus, and the Work-Bench made with a Whisper 200 alternator, an induction machine, and a variable frequency inverter.

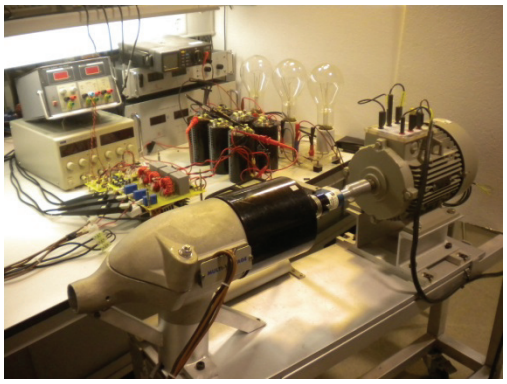

Fig.8. Prototype, DC-Bus and Wind-Bench

Two different experiments have been carried out. During first experiment, shown at Fig.9a-9b, 1.4 kW are delivered to the DC-Bus with a steady voltage of V_b=320 V. During second experiment, depicted in Fig. 10c, the DC-Bus changes slowly, during 75ms, from V_b=285 V to V_b=355 V.

In the first experiment, when the wind generator is stopped, the power-supply feeds the load, delivering 5.32 A at 320 V. When the generator begins to turn, the current given by the power supplies progressively decreases, until a minimum value of 1.2 A is reached. At this point, the power injected to the microgrid is slightly over 1.3 kW.

As can be seen at Fig.9a, the input currents have a good sinuousidal shape. There are slight differences in amplitude, due to small differences in conductance g_1, g_2, g_3 values.

In oscilloscope caption of Fig.9b, we can appreciate one of the inductor currents I_L, as well as its reference signal, that is proportional, to the rectified input voltage. Inductor ripple current is negligible because the oscilloscope is working in the "Average" mode.

The transient experiment is shown at Fig.9c. The bus voltage slope during the transient, is defined by the capacitor bank C_b and the maximum available current, 20 A.

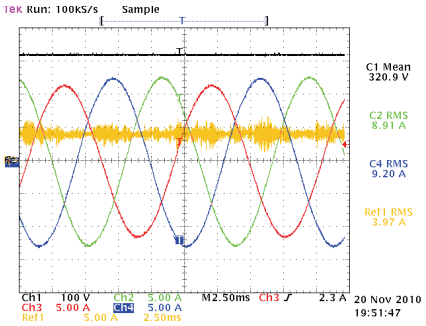

Fig.9a. Steady Bus Experiment

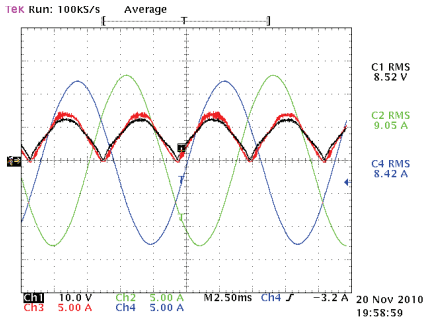

Fig.9b. I_L and V_{ref} Details, Steady Bus

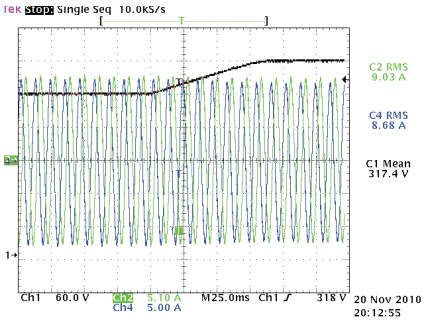

Fig.9c. DC-Bus Voltage Transient

As the converter presented in this work should perform like a power source, if the bus voltage increases, the current injected in the bus must decrease, and the converter power would remain unchanged. Therefore, the converter input currents should remain constant for any bus voltage. The caption at Fig.9c shows a good agreement between practical results and theoretical hypothesis, as the converter input currents remain practically constant.

Conclusions

In this work, three-phase modular PFC's developed from single-phase boost PFC circuits are investigated.

When a single-phase boost PFC is connected in a poly-phase system without isolation either at the input, or at the output, balancing problems among input currents appear.

To avoid these undesired interactions, diverse techniques can be found in the literature. Magnetic coupling has been introduced to enhance the isolation among phases, mainly due to the transformer effect, forcing the input and output wire currents to be equal. Besides, magnetic coupling incorporates also other improvements like losses, cost, and weight reduction. Namely, the number of magnetic cores can be halved if compared to previous approaches.

To assure good sinusoidal waveforms, sliding mode control and Loss-Free Resistor concepts have been considered. Good experimental waveforms corroborated our analysis.

Acknowledgment: This work has been partially sponsored by the Spanish Ministry of Research and Science, under grants: DPI2009-14713-C03-02, and Consolider RUE CSD2009-00046.

REFERENCES

[1] Corin Millais, Luisa Colasimone, "*Large Scale Integration of Wind Energy in the European Power Supply: Analysis Issues and Recommendations*", Report of The European Wind Energy Association (EWEA), 2005.

[2] Valderrama-Blavi, H., Bosque-Moncusi, J.M., Marroyo, L., Guinjoan, F., Barrado, J.A.; Martinez-Salamero, L., "*Adapting a low voltage PEM fuel-cell to domestic grid-connected PV system*," Industrial Electronics, 2009. IECON '09. 35th Annual Conference of IEEE, vol., no., pp.160 165, 3-5 Nov. 2009.

[3] Kyohei Kuroane, Tomonobou Senjyu, Atsushi Yona, Naonitsu Urasaki, Endusa Billy Muhando, Toshihisa Funabashi, "*A High Quality Power Supply System with DC Smart Grid*," Transmission and Distribution Conference and Exposition, 2010 IEEE PES, vol., no., pp. 1 - 6, 19-22 April 2010.

[4] Lee, F.C.; Barbosa, P.; Peng Xu; Jindong Zhang; Bo Yang; Canales, F.; , "*Topologies and design considerations for distributed power system applications*," Proceedings of the IEEE , vol.89, no.6, pp.939-950, Jun 2001.

[5] Alahuhtala, J., Tuusa, H., "*Four-Wire Unidirectional Three Phase /Level / Switch (VIENNA) Rectifier*," IEEE Industrial Electronics, IECON 2006 - 32nd Annual Conference on , vol., no., pp.2420-2425, 6 10 Nov. 2006.

[6] Heldwein, M.L.; Ferrari de Souza, A.; Barbi, I.; , "*A simple control strategy applied to three-phase rectifier units for telecommunication applications using single-phase rectifier modules* ," Power Electronics Specialists Conference, 1999. PESC 99. 30th Annual IEEE , vol.2, no., pp.795-800 vol.2, 1999.

[7] Spiazzi, G., Lee, F.C., "*Implementation of single-phase boost power-factor-correction circuits in three-phase applications*," Industrial Electronics, IEEE Transactions on , vol.44, no.3, pp.365-371, Jun 1997.

[8] Jaehong Hahn, Enjeti, P.N., Pitel, I.J. , "*A new three-phase power-factor correction (PFC) scheme using two single-phase PFC modules*," Industry Applications, IEEE Transactions on , vol.38, no.1, pp.123-130, Jan/Feb 2002.

[9] Calvente, J., Martinez-Salamero, L., Valderrama, H., Vidal-Idiarte, E., "*Using magnetic coupling to eliminate right half-plane zeros in boost converters*," Power Electronics Letters, IEEE , vol.2, no.2, pp. 58- 62, June 2004.

[10] Sable, D.M., Cho, B.H., Ridley, R.B., "*Elimination of the positive zero in fixed frequency boost and flyback converters*," Applied Power Electronics Conference and Exposition, 1990. APEC '90, Conference Proceedings 1990., Fifth Annual , vol., no., pp.205-211, 11-16 Mar 1990.

[11] Milanovic, M., Mihalic, F., Jezernik, K., Milutinovic, U., "*Single phase unity power factor correction circuits with coupled inductance*," Power Electronics Specialists Conference, 1992. PESC '92 Record., 23rd Annual IEEE , vol., no., pp.1077-1082 vol.2, 29 Jun-3 Jul 1992.

[12] Slobodan Cuk, "*DC-to-DC switching converter with zero input and output current ripple and integrated magnetics circuits".* United States Patent 4,257,087, from March 17, 1981.

[13] Sira-Ramirez, H., "*Sliding motions in bilinear switched networks*," Circuits and Systems, IEEE Transactions on , vol.34, no.8, pp. 919- 933, August 1987.

***Authors**: eng. Freddy Flores-Bahamonde, freddy.flores@urv.cat; Dr. Hugo Valderrama-Blavi, hugo.valderrama@urv.cat; Mr. Josep Maria Bosque-Moncusí, josepm.bosque@urv.cat; Prof. Luis Martinez-Salamero, luis.martinez@urv.cat; Mr. Antonio Leon-Masich, antonio.leon@urv.cat; Dr. José Antonio Barrado, joseantonio.barrado@urv.cat, GAEi (Automatic and industrial Electronic Group) Laboratory, DEEEiA Department from Rovira i Virgili University, Av. Paisos Catalans 26, 43007, Tarragona, Spain.*